PERGAMON

International Journal of Solids and Structures 36 (1999) 1311–1327

INTERNATIONAL JOURNAL OF SOLIDS and STRUCTURES

On the response of curved laminated panels subjected to transverse impact loads

Laura S. Kistler[1], Anthony M. Waas[2,*]

Composite Structures Laboratory, Department of Aerospace Engineering, University of Michigan, Ann Arbor, MI 48109-2140, U.S.A.

Received 27 March 1997; in revised form 18 December 1997

Abstract

Using static response characteristics as a tool for understanding impact response, the influence of in-plane and out-of-plane boundary conditions, the effect of curvature, and the validity of linear and nonlinear plate theory are investigated for the transverse central impact on thin fiber reinforced composite cylindrical panels. Comparisons between the force-deformation curves of a low velocity impact response and static problem are made. These curves illustrate the importance of nonlinear effects on the large deformation response, including the influence of curvature. The static response is a lower limit to the impact response and, for the present circumstances, can give insight into low velocity impact response behavior.

1. Introduction

The present analysis of cylindrically curved laminated panels, supported with experimental data, illustrates the sensitivity of large deformation impact response to a variety of modeling assumptions and physical parameters. The effect of impactor velocity, panel curvature, thickness, both in-plane and out-of-plane boundary conditions and the validity of linear and nonlinear plate theory on the resulting impact force and panel displacement is investigated, especially in the context of impact.

Low velocity impact refers to situations where the target response can be approximated as quasi-static and the impactor, which always behaves dynamically is modeled as a rigid body. The present research is concerned with an impact event of moderate severity in which both the local nonlinear force-deformation contact and the global behavior of plate flexure, stretching and vibration are considered to dominate the structural response.

* Corresponding author.

[1] Graduate Research Assistant, currently with Boeing Commercial Airplane company, Seattle.

[2] Associate Professor.

0020–7683/99/$ - see front matter
PII: S0020–7683(98)00005–5

Table 1
Experimental data for test matrix, 8 Plies

Case	Plies	Radius (m)	Energy (N m)	B.C.	Max Force (N)	Max Displ. (mm)	Contact (ms)
1	8	0.381	0.68	ccss	230		18.7
2[a]	8	0.381	1.02	ccss	348	6.5	17.0
3[a]	8	0.381	1.36	ccss	417	6.0	15.2
4(a)	8	0.381	0.68	cccc	216	3.3	14.4
4(b)	8	0.381	0.68	cccc	223		14.1
5	8	0.381	1.02	cccc	341	3.5	13.5
6[a]	8	1.524	1.02	ccss	431	4.2	13.8
7[a]	8	1.524	1.36	ccss	501	4.9	12.5
8[a]	8	1.524	1.69	ccss	584	4.8	11.6
9	8	1.524	0.68	cccc	341	3.4	12.4
10	8	1.524	1.02	cccc	438	4.6	12.8

[a] C-scanned

Cylindrically curved test specimens, 25.4 cm (10 in) in axial direction and 12.7 cm (5 in) in arc length, were fabricated with Hercules, Inc. AS4 graphite fiber tape and 3502 epoxy resin. The quasi-isotropic panels had 8, 16, or 24 plies with an average thickness of approximately 1 mm, 2 mm, and 3 mm, respectively. Specimens were made for two radii of curvature, 0.381 m (15 in) and 1.524 m (60 in). Instrumented with a force transducer, a fixed 1.13 kg (2.5 lb) mass with a 12.7 mm (0.5 in) diameter steel hemispherical tip was dropped from varying heights. Measurements of the panel center deflections were obtained with a fiber optic displacement sensor. The curved ends of the panel were sandwiched between two curved surfaces creating a clamped condition. The straight edges were constrained by either clamped supports or knife-edges. The choice of test matrices (Tables 1, 2 and 3) were motivated by the availability of results for flat laminated plates, with similar stacking geometry as has been considered here, reported by Ambur et al. (1993) and Prasad et al. (1994).

Classical lamination theory and the strong bending of shells formed the basis of a derivation for a nonlinear system of equations. With the impact loading described in terms of Hertz' contact law and an assumed modes approximation, the impact force and shell motion was solved for as a function of time using a Runge-Kutta solution method. Furthermore, an ABAQUS finite element model, with and without geometric nonlinearity, was used to study the dynamic response of the panel as reported in [2]. Details of the experimental impact tests, a large deformation assumed mode analysis, and an ABAQUS finite element analysis have been presented elsewhere (Kistler, 1994, 1996; Kistler and Waas, 1997a), and are omitted here for the sake of brevity. The interested reader is referred to these publications for additional details. Previous work related to the present study was reported by Matsuhashi et al. (1993) who compared linear and nonlinear model predictions with impact test data for flat laminates, while the impact damage resistance of several laminated material systems was investigated by Lagace and Wolf (1995). One of the first studies

Table 2
Experimental data for test matrix, 16 Plies

Case	Plies	Radius (m)	Energy (N m)	B.C.	Max Force (N)	Max Displ. (mm)	Contact (ms)
11	16	0.381	0.68	ccss	431	—	7.4
12[a]	16	0.381	1.36	ccss	557	2.6	7.2
13	16	0.381	2.04	ccss	737	—	7.7
14[a]	16	0.381	2.71	ccss	863	4.6	7.7
15[a]	16	0.381	3.39	ccss	1016	4.2	7.7
16[a]	16	0.381	4.07	ccss	1099	4.4	7.7
17(a)	16	0.381	0.68	cccc	515	1.6	5.7
17(b)	16	0.381	0.68	cccc	557	—	5.4
18	16	0.381	1.36	cccc	696	2.4	5.9
19(a)	16	0.381	2.04	cccc	821	3.0	6.0
19(b)	16	0.381	2.04	cccc	877	—	5.9
20	16	0.381	2.71	cccc	974	3.7	6.7
21	16	0.381	3.39	cccc	1085	4.2	6.1
22	16	1.524	1.36	ccss	682	2.8	7.4
23	16	1.524	2.04	ccss	877	3.4	7.1
24	16	1.524	2.71	ccss	1085	3.8	7.0
25(a)	16	1.524	3.39	ccss	1224	4.0	6.7
25(b)[a]	16	1.524	3.39	ccss	1183	3.6	7.2
26	16	1.524	0.68	cccc	543	1.8	6.3
27	16	1.524	1.36	cccc	765	2.3	6.2
28	16	1.524	2.04	cccc	988	2.8	6.0
29	16	1.524	2.71	cccc	1183	3.2	6.0
30	16	1.524	3.39	cccc	1350	3.2	6.0

[a] C-scanned

that investigated impact response of flat composite panels was reported by Sun and Chattopadhyay (1975) who set the pace for much of the work to follow. The results presented here complement the findings of the previous studies and examines in detail the effects of panel curvature and boundary conditions on the panel response. A study that examines the influence of both these effects simultaneously in the context of impact of curved panels is novel and points to the significance of nonlinear effects that manifest through geometric nonlinearity and inplane edge boundary conditions.

During the course of our investigations, it was observed that the flatter panels responded to impact with larger peak forces than more curved panels, as well as smaller peak displacements and contact durations. And yet, near certain impact energies, some panels did not exhibit any dependence on curvature. Difficulty in reconciling the experimental test data with various analytical results lead to the present study. A relationship between static and dynamic response behavior is sought as a tool for understanding the impact response of curved laminated panels subjected to transverse loads.

Table 3
Experimental data for test matrix, 24 Plies

Case	Plies	Radius (m)	Energy (N m)	B.C.	Max Force (N)	Max Displ. (mm)	Contact (ms)
31(a)	24	0.381	0.68	ccss	800	1.1	4.1
31(b)	24	0.381	0.68	ccss	807	—	4.1
32	24	0.381	1.36	ccss	1169	1.6	4.1
33(a)	24	0.381	2.04	ccss	1419	2.1	4.1
33(b)	24	0.381	2.04	ccss	1350	—	4.1
34	24	0.381	2.71	ccss	1600	2.4	4.1
35	24	0.381	3.39	ccss	1774	2.7	4.2
36(a)	24	0.381	0.68	cccc	737	1.1	3.4
36(b)	24	0.381	0.68	cccc	918	—	3.4
36(c)	24	0.381	0.68	cccc	918	—	3.4
37	24	0.381	1.36	cccc	1224	1.4	3.8
38(a)	24	0.381	2.04	cccc	1461	1.8	3.9
38(b)	24	0.381	2.04	cccc	1545	—	3.6
39	24	0.381	2.71	cccc	1670	2.0	3.9
40	24	0.381	3.39	cccc	1878	2.3	3.9
41	24	1.524	0.68	ccss	765	1.1	4.3
42	24	1.524	1.36	ccss	1099	1.7	4.3
43	24	1.524	2.04	ccss	1391	2.2	4.2
44	24	1.524	2.71	ccss	1635	2.4	4.3
45	24	1.524	3.39	ccss	1878	2.7	4.1
46	24	1.524	0.68	cccc	800	1.0	3.9
47	24	1.524	1.36	cccc	1169	1.6	3.8
48	24	1.524	2.04	cccc	1419	1.7	3.8
49	24	1.524	2.71	cccc	1670	2.1	3.8
50	24	1.524	3.39	cccc	1878	2.2	3.8

2. Impact tests

The sketch in Fig. 1 shows the coordinate system (x, s, z) and respective displacements (u, v, w) of the cylindrical panel. The dimensions are denoted as: axial length, a, arc length, b, thickness, h, and radius of curvature, r. The panel height, H, is the height of the crown from the supports and is similar to an arch rise parameter.

Tables 1, 2 and 3 list the number of plies, radius of curvature, impact energy, boundary condition, maximum impact force, maximum center displacement, and contact duration for the entire test matrix. The boundary condition notation is as follows: CCSS, clamped curved edge and simple (knife) straight edge supports; CCCC, all clamped edge supports. The contact duration listed is the time at which the force returns to zero, however, this is not usually the time at which the displacement returns to zero. Experimental data reflect the results of individual tests, not averages of multiple tests.

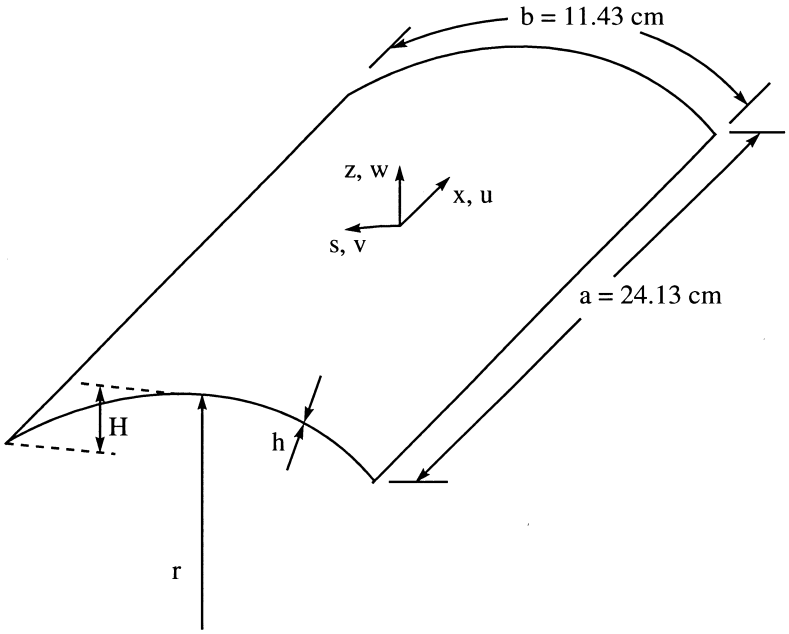

Fig. 1. Coordinate system and nomenclature.

3. Impact response relation to static response

For the study of large deformation impact response of thin, cylindrically curved panels, the local nonlinear force-deformation contact and the global behavior of plate flexure, stretching and vibration have been considered to dominate the structural response in the present dynamic model. However, when the mass of the impactor is large compared with the equivalent mass of the panel, the panel velocity is low enough to neglect through-the-thickness stress wave effects. The material used in the present study is strain rate insensitive and therefore the target is modeled as an elastic material and statically determined contact laws are used to model the local indentation, which is also assumed strain rate independent.

In addition, it can also be assumed that the panel material is not strain-rate sensitive, and since the panel is thin, such that the local indentation is small compared with the global response, then the impact response should approach an equivalent static response. A straightforward way to check whether the conditions set forth in the experimental tests meet these criteria is to compare the force-deformation curves of a low velocity impact and static problem. This curve can be used to illustrate the importance of nonlinear effects including the influence of curvature.

To examine the impact to static relationship, the experimental data from Case 2 and Case 6 of the text matrix will be compared with the linear and nonlinear analytical results as well as the results from a static finite element (FE) analysis. The out-of-plane boundary conditions are clamped in the x direction and simply supported in the s direction. The in-plane boundary conditions are such that the tangential motion is fixed while the normal motion remains free. In the FE model, the solution procedure is either dynamic, such that a sphere with initial velocity

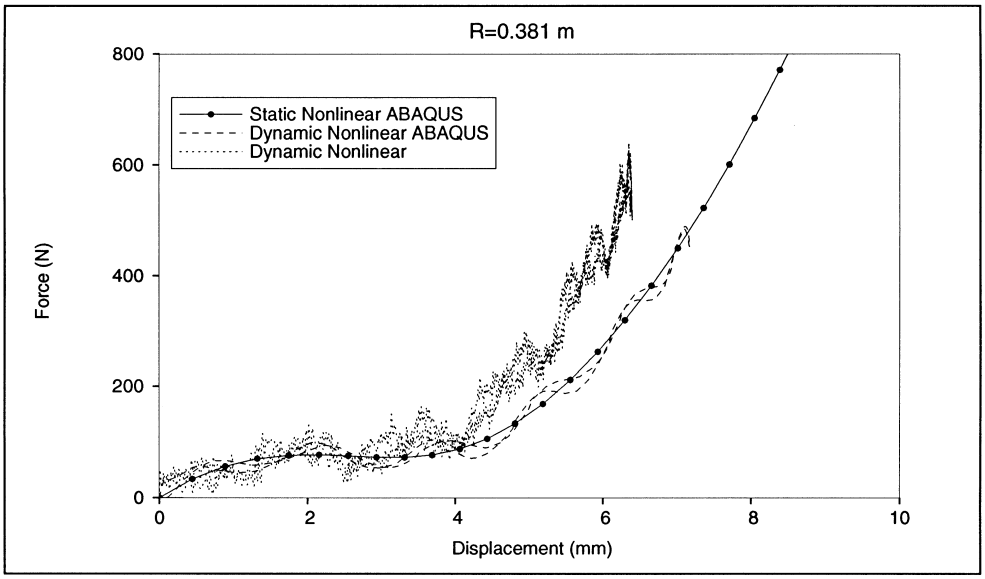

(a) $R = 0.381\text{m}$ CASE 2

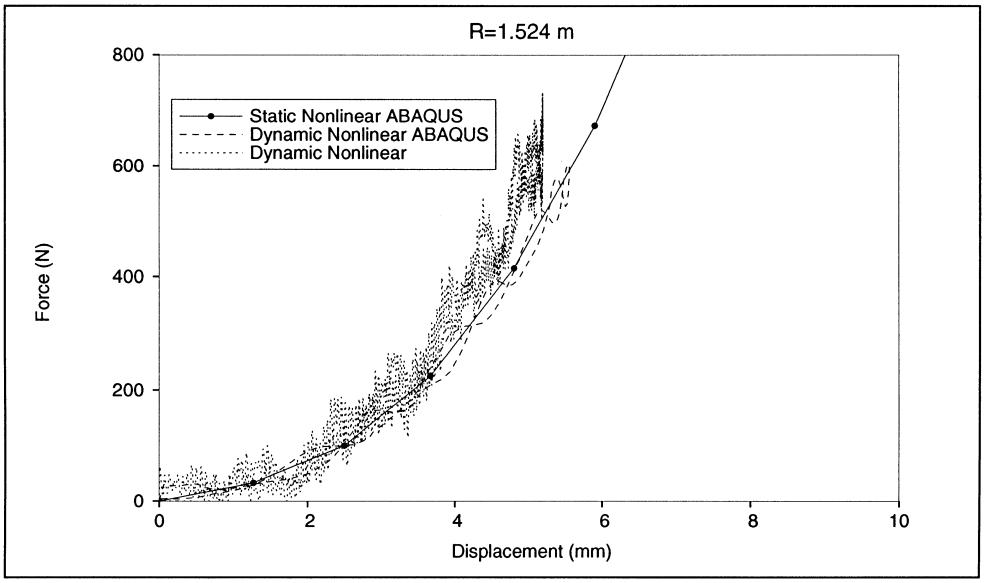

(b) $R = 1.524\text{m}$ CASE 6

Fig. 2. Nonlinear impact response relation to static response.

transversely impacts the shell, or static, such that a point load is applied at the panel center with the load magnitudes found as part of the solution.

Force versus displacement plots are shown in Figs 2–4 for the 0.381 m and 1.524 m radius, 8 ply

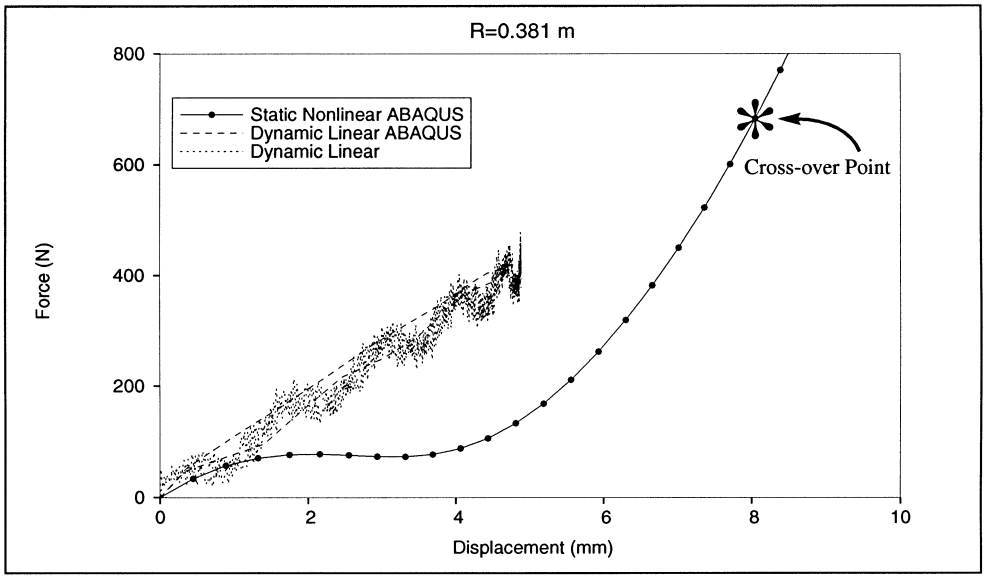

(a) $R = 0.381\text{m}$ CASE 2

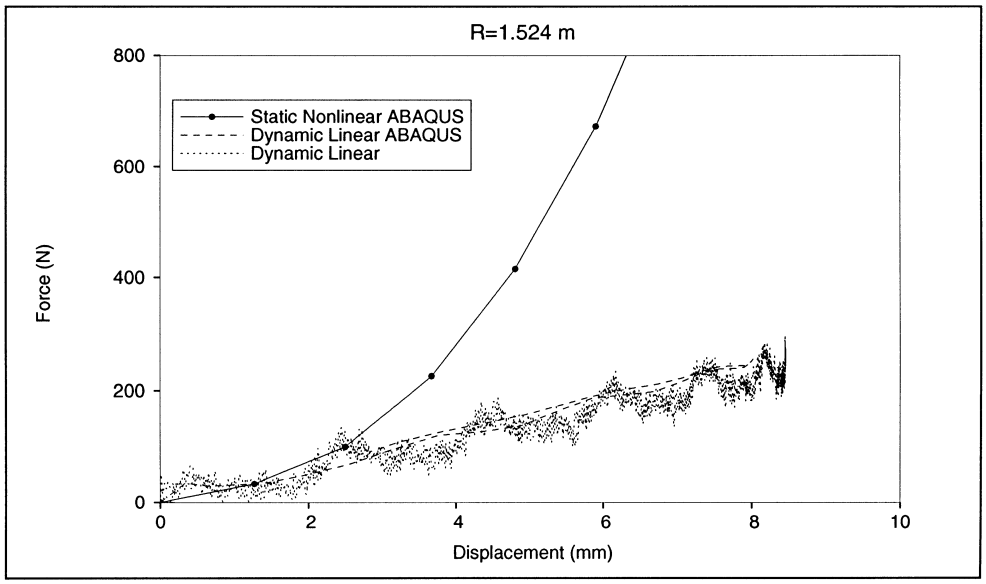

(b) $R = 1.524\text{m}$ CASE 6

Fig. 3. Linear impact response relation to static response.

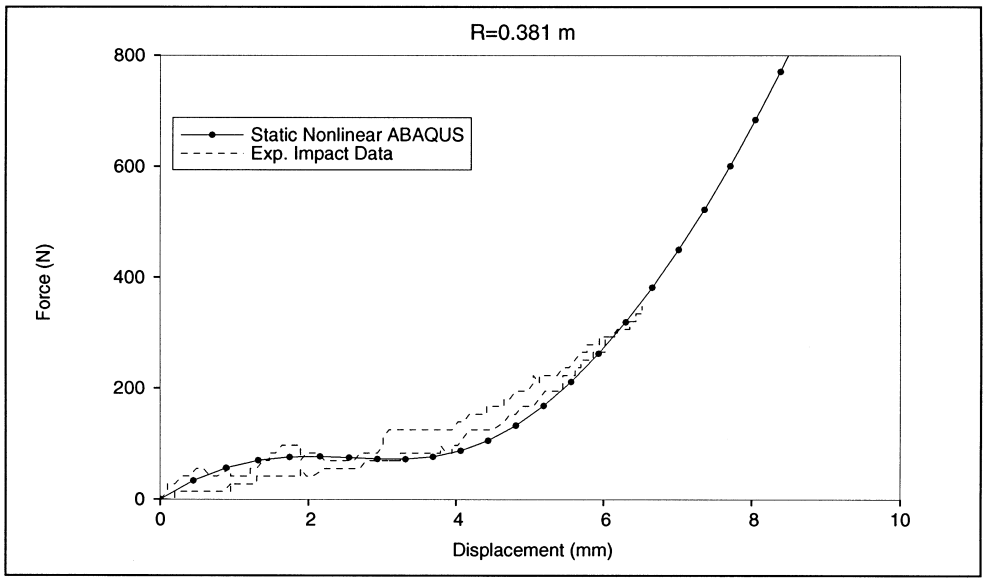

(a) $R = 0.381\text{m}$ CASE 2

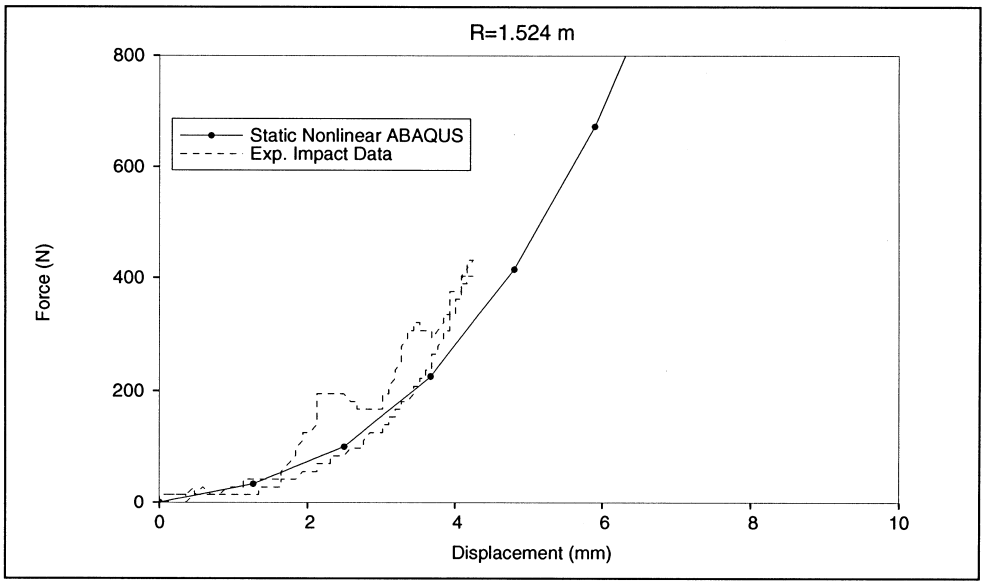

(b) $R = 1.524\text{m}$ CASE 6

Fig. 4. Experimental impact response relation to static response.

panels. In these figures the labels refer to a nonlinear assumed mode analysis reported in Kistler and Waas (1997a) and the nonlinear static FE analysis. The impact response predicted by the nonlinear analyses closely follows the nonlinear static model for both cases (Fig. 2). Obviously, the dynamic response includes vibrations, but the general behavior remains the same. The static response is a lower limit to the impact response and for these circumstances can give insight into the impact response. All of the dynamic responses show a low frequency content overlayed with a high frequency signal. As has been conclusively shown earlier via a 3D FE analysis (Murphy, 1994), these high frequency content in the force-time plots are due to the local bending of the panel around the contact area with the impactor. In the present work, maximum numerical damping was used to eliminate some of the high frequency content in the FE analysis. This was done in order to facilitate obtaining a converged solution. In the experiment, both the displacement and force outputs were fed a signal conditioning stage followed by a low pass wide band filter. Thus, in comparing the results of the assumed mode analysis with the experimental and FE results, the absence of some of the high frequency content is to be expected.

The difference between the linear and nonlinear curves further illustrates the response regime beyond which a nonlinear analysis is required. While the linear analyses adequately model the response for small deformations, the deformation response follows the initial slope of the nonlinear force-displacement curve and therefore, underpredicts the stiffness of the flatter 1.524 m panel and overpredicts the stiffness of the more curved 0.381 m panel at this impact energy (Fig. 3). Although a linear analysis of these panels with these boundary conditions will always underpredict the stiffness of the large deformation response in the flatter panel (and also flat plates), in the more curved panel there exists a cross-over point below which the stiffness will be overpredicted by a linear analysis and above which the stiffness will be underpredicted. The approximate cross-over point between the linear and nonlinear result is marked by an '*' on Fig. 3(a).

Perhaps the most interesting consequence of comparing the force-displacement curves for these two panels is that the influence of curvature on the response can be clearly identified for a fixed thickness, boundary condition, and impact energy. Such a comparison is as indicated in Fig. 4. In the small deformation regime, the more curved, 0.381 m radius panel is more stiff (indicated by a higher slope) than the shallower panel. However, as the displacement increases, the shallower, 1.524 m panel increases in stiffness while the more curved panel first softens, then stiffens. The more curved panel exhibits a limit-point instability similar to a clamped arch with a transverse point load at its center. A limit-point instability occurs when the load increases until the panel deflects through some critical amount, after which the load relaxes, until the panel resists the motion in its inverted state. The 1.524 m radius panel has an arch height of nearly 1 mm while the 0.381 m radius panel has an arch height of 4.3 mm. For this geometry and boundary conditions, the shallower panel does not show evidence of a limit-point, rather, it behaves more like a flat plate and is almost immediately perturbed beyond its arch height to a peak displacement that is relatively large, beyond three times its panel height. The more curved panel, on the other hand, bends and stretches as the deformation approaches its panel height to a peak displacement that is relatively small, just beyond one of its panel heights.

Now consider how the response behavior varies with velocity as well as curvature. Consider the all clamped, 16 ply panels impacted at 0.68 N m or 3.39 N m, corresponding to Cases 17, 21, 26 and 30 of the test matrix. For both the 0.381 m and 1.524 m radius panels, Fig. 5(a) shows the

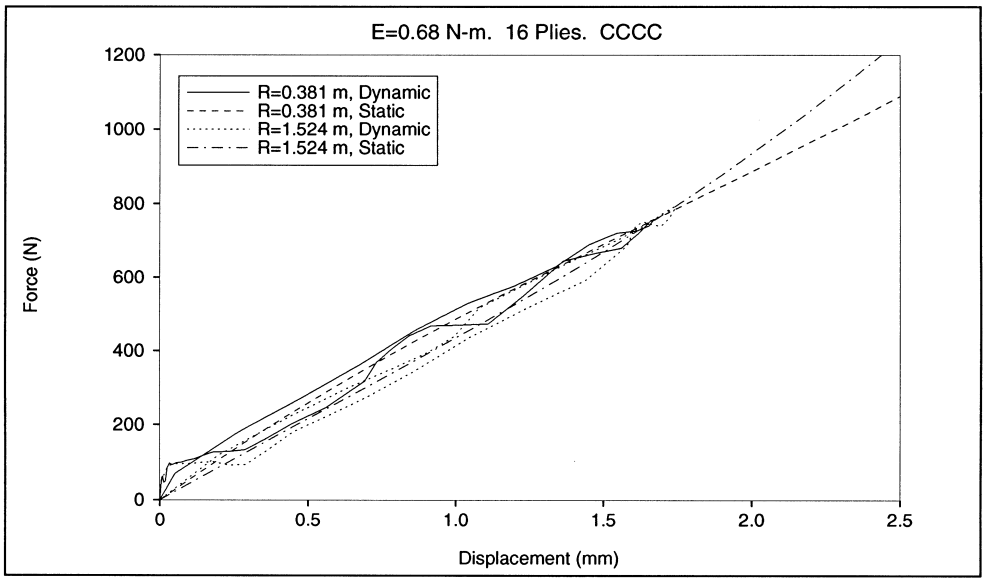

(a) $E = 0.68$N-m CASES 17, 26

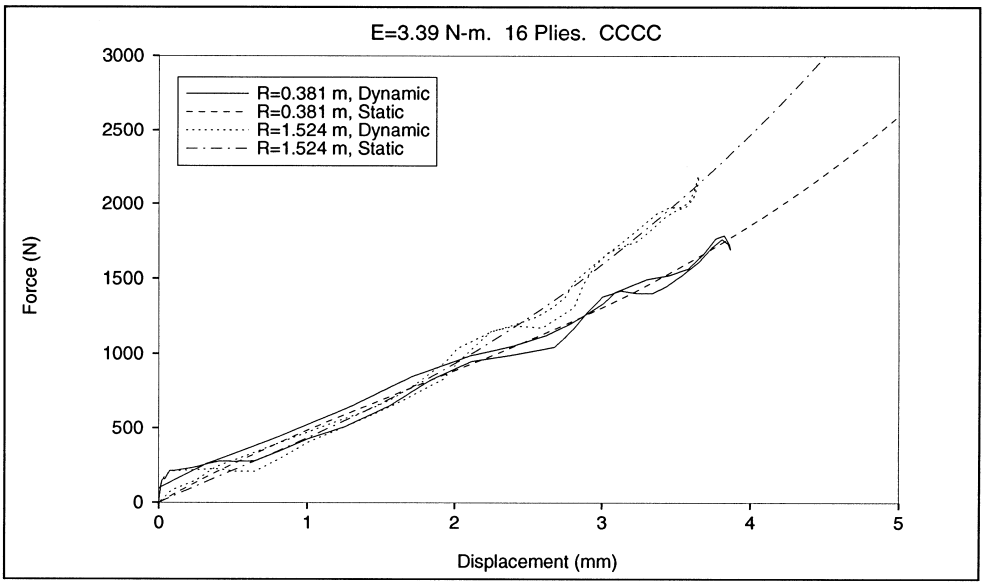

(b) $E = 3.39$N-m CASES 21, 30

Fig. 5. Influence of velocity and curvature, 16 Plies.

dynamic nonlinear FE force-displacement curves for an impact energy of 0.68 N m along with the static nonlinear FE force-displacement curves. Near this impact energy the resultant peak response of panels (both radii) corresponds to a cross-over point in the static force-displacement curve.

Without knowledge of the static curves or other impact energy data, it appears that the impact response of these panels does not appear to depend significantly on curvature. For a higher impact energy of 3.39 N m, Fig. 5(b) shows the dynamic nonlinear FE force-displacement curve for both panels along with the corresponding static nonlinear FE force-displacement curves. At this impact energy, the resultant peak force of the shallower panel is higher than the more curved panel, supporting the behavior observed in the 8 ply CCSS panels.

To further illustrate the influence of velocity and curvature on the impact response, consider the CCSS 24 ply panels impacted at 0.68, 2.04, or 3.39 N m, corresponding to Cases 31, 33, 35, 41, 43 and 45 of the test matrix. Figure 6 shows the dynamic nonlinear FE force-displacement curves for the three impact energies along with the corresponding static curves. At 2.04 N m impact energy, the resultant peak response of both panels corresponds to the cross-over point in the static force versus deformation curve. Below this point, as seen in the 0.68 N m impact energy, the resultant peak force of the shallower panel is lower than the more curved panel. Above this point, the opposite behavior is observed as seen in the 3.39 N m impact energy where the resultant peak force of the shallower panel is higher than the more curved panel and again supports the behavior that shallower panels can exhibit stiffer response behavior than more curved panels.

Although curvature may introduce structural response behavior similar to the limit-point instability of an arch, the present nonlinear analyses account for large deformations and in-plane membrane effects and are able to accurately predict this behavior in the panels under investigation. Furthermore, for these cases the nonlinear dynamic force-displacement curves correspond well with the nonlinear static response (with vibrations superimposed).

4. Effect of boundary conditions

Although the panels under consideration are midplane symmetric and the bending and stretching response is not coupled through the material coupling rigidities B_{ij}, the in-plane membrane forces N_x, N_s and N_{xs} are coupled to the large deformation out-of-plane motion through the squares of the plate slopes and to the out-of-plane displacement through the w/r term of the nonlinear strain displacement relations. The strain-displacement relations also include the slopes of the in-plane displacements. Therefore it is essential that not only the transverse displacements and boundary conditions are properly modeled, but also the in-plane displacements and boundary conditions. Since matching the actual impact test boundary supports with analytically assumed conditions is not a simple task, many test cases have been run to identify how the boundary conditions, and hence the assumed mode shapes in the analytical model, affect the response of the panel.

4.1. *In-plane boundary conditions*

While holding the out-of-plane boundary conditions constant, the in-plane boundary conditions are varied for three cases: (i) all in-plane displacements equal to zero, labeled 'In Fixed'; (ii) all in-plane forces equal to zero, labeled 'In Free'; and (iii) tangential displacements equal to zero and normal forces equal to zero, labeled 'Mixed'. Whereas the axial beam vibration mode shapes exactly satisfy the in-plane displacement boundary conditions, the in-plane force boundary conditions cannot be satisfied by the axial beam vibration mode shapes. The displacement formulation

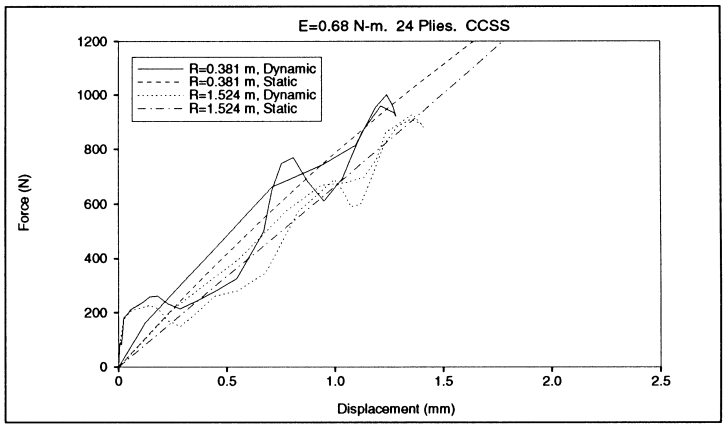

(a) $E = 0.68$N-m CASES 31, 41

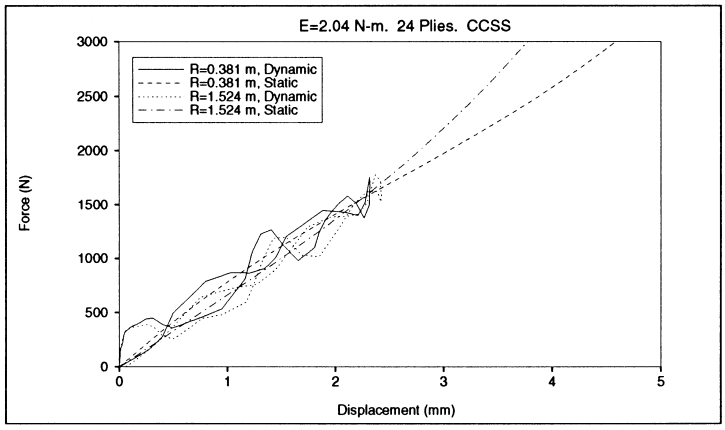

(b) $E = 2.04$N-m CASES 33, 43

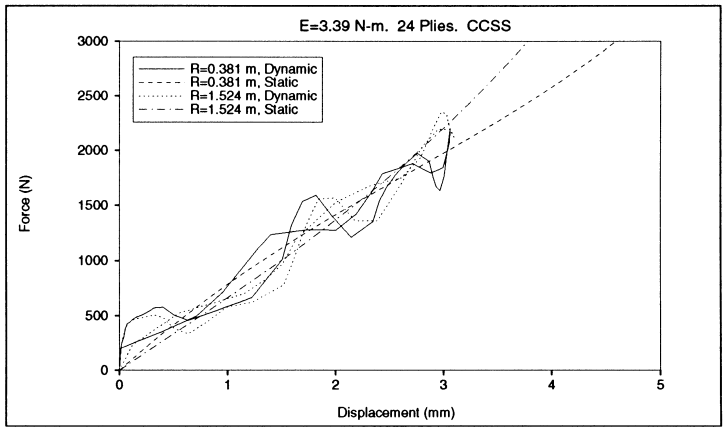

(c) $E = 3.39$N-m CASES 35, 45

Fig. 6. Influence of velocity and curvature, 24 Plies.

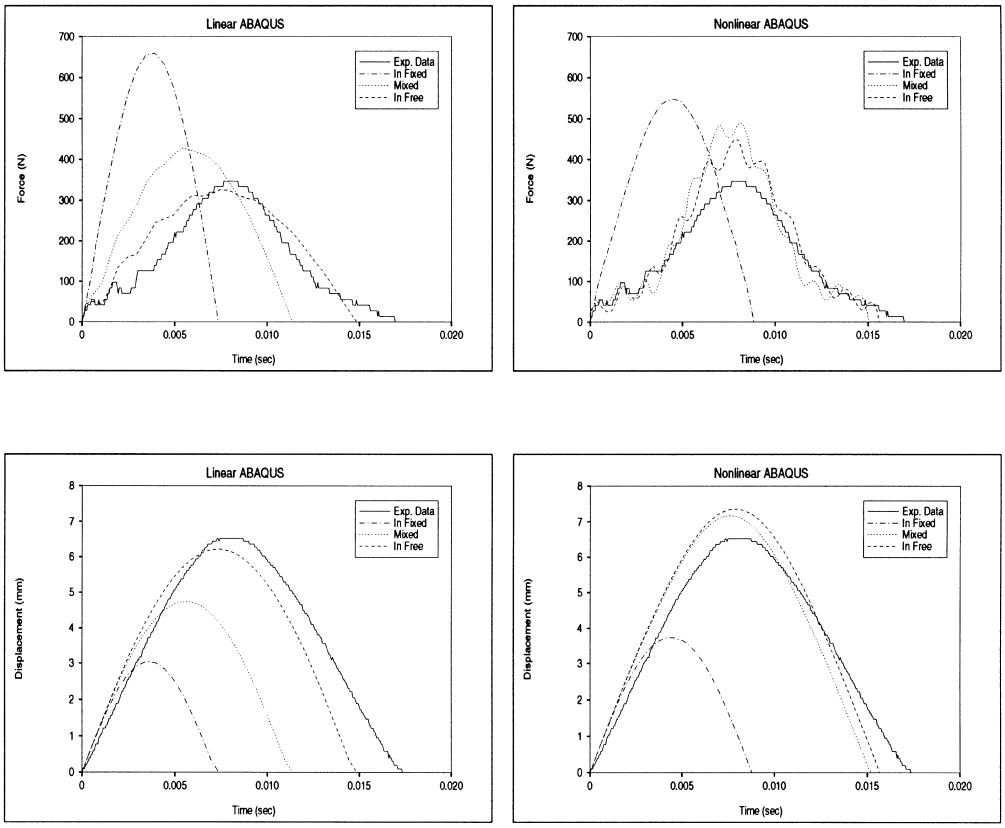

Fig. 7. Inplane boundary effect on response histories, Case 2.

of this analysis is appropriate for in-plane displacement boundary conditions, whereas a stress function formulation would be preferred for cases involving in-plane force boundary conditions. The FE model is not based on assumed mode shapes and so all three in-plane boundary condition cases can be exactly modeled in a discretized sense. Since the FE model generates results similar to the analytical model and the FE formulation can model every in-plane boundary condition, only results of the FE model will be presented here.

To facilitate comparisons, every result reported so far has prescribed the in-plane boundary condition as Mixed. A panel's impact force and displacement response can depend significantly on the in-plane boundary conditions. The In Fixed case should be an upper bound with respect to in-plane stiffness while the In Free case should be a lower bound. The experimental results should fall in between these bounds assuming the out-of-plane boundary conditions (and every other parameter) is modeled exactly.

Consider an 8 ply panel with a 0.381 m radius, impacted at 0.68 N m of energy, clamped on the curved edges and simply supported on the straight edges (Case 2). Figure 7 shows how in-plane boundary conditions in the linear and nonlinear FE model affect the impact force and displacement response histories. As the in-plane boundary condition varies toward an increased restraint of

the in-plane motion, the panel response will exhibit higher peak impact forces, smaller peak displacements, and shorter contact durations. The similarity of the Mixed and In Free response in the nonlinear analysis suggests that the response is not influenced by the tangential restraints as much as the normal restraints. Although the In Free response of the linear analysis predicts a peak impact force, peak displacement, and contact duration close to the experimental data, the nonlinear In Free analysis most closely matches the experimental data with respect to the shape of its force history curve. In the first 5 ms, the In Free displacement history is essentially linear for both analyses, however, as demonstrated in Section 3 the force history predicted by the linear analysis increases linearly while the force history of the nonlinear analysis first increases, softens, then increases again in conformity with the limit-point instability associated with this case.

The experimental impact data are indeed roughly bounded by the nonlinear response predicted by the In Fixed and In Free boundary conditions. Since a static analysis has been shown to provide insight toward understanding impact response behavior, static force-displacement curves for both radii of curvature are shown in Fig. 8 with all three in-plane boundary conditions and CCSS out-of-plane boundary conditions. For both panels, the in-plane boundary conditions significantly influence the response. The most unusual influence is on the In Fixed case, 0.381 m radius panel which responds almost linearly then softens only after it has deformed by more than 1.5 times its panel height.

For every thickness of the more curved panels, the in-plane tangential boundary conditions do not influence the response as much as the in-plane normal boundary conditions as can be seen by the greater difference between the In Fixed and Mixed response as well as the similarity between the Mixed and In Free response of the static force-displacement curves. In the flatter panels, however, the in-plane tangential boundary conditions can influence the response as much as the in-plane normal boundary conditions.

4.2. *Out-of-plane boundary conditions*

While holding the in-plane boundary conditions constant, the out-of-plane boundary conditions are varied for three cases: (i) all clamped edges, CCCC; (ii) all simply supported edges, SSSS; and (iii) curved edges clamped and straight edges simply supported, CCSS. Consider again the 8 ply panel with a 0.381 m radius, impacted with 0.69 N m of energy, with the in-plane boundary condition taken as Mixed. The nonlinear analyses tend to over predict the experimental data. Of the two proposed causes, boundary conditions and velocity, the influence of both parameters is shown in Fig. 9. The SSSS response is not shown because its response is similar to the CCSS response for the case in consideration, suggesting that the response is not influenced by the curved edge restraints as much as the straight edge restraints. Recall that the panels under consideration are twice as long in the axial direction as in the curved direction and so the geometry accordingly makes the influence of the straight edge out-of-plane boundary conditions larger than the curved edge out-of-plane boundary conditions.

As the out-of-plane boundary condition varies toward an increase in restraint in edge rotations, the panel response will exhibit higher peak impact forces, smaller peak displacements, and shorter contact durations. For both panels ($r = 0.381$ m or 1.524 m), the 0.68 N m nonlinear FE analysis predicts a force history which agrees very well in shape and magnitude with the experimental impact energy of 1.02 N m indicating that the actual test velocity may indeed be lower than the value used in the analysis. While the 0.68 N m nonlinear FE analysis predicts a displacement

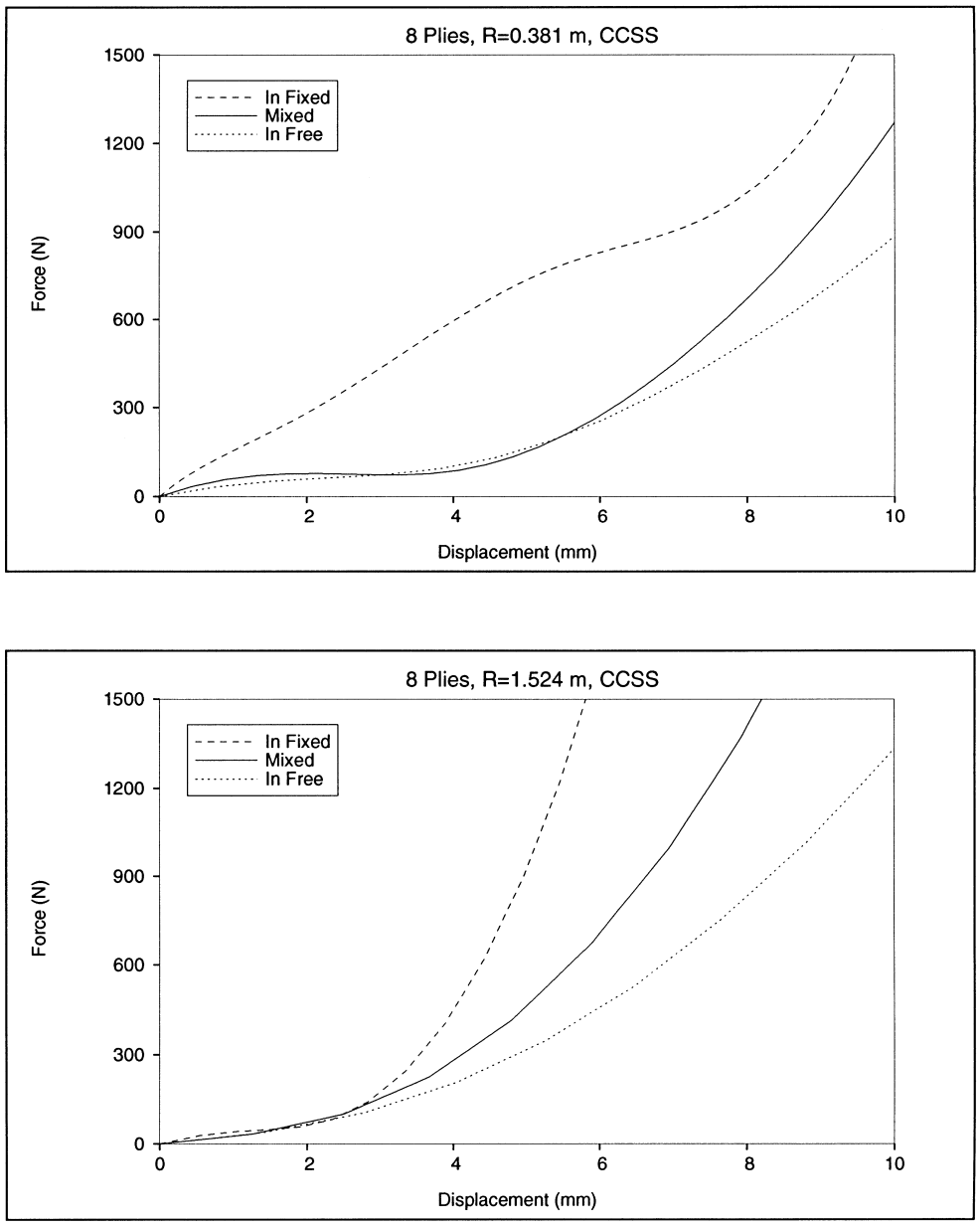

Fig. 8. Inplane boundary effect on static response.

history which also agrees very well with the experimental impact energy of 1.02 N m for the CCSS out-of-plane boundary conditions, the agreement is not as good for the CCCC condition. Inspection of the CCCC 1.02 N m experimental displacement curve indicates that the signal may be inaccurate since its shape is not uniformly parabolic near its peak.

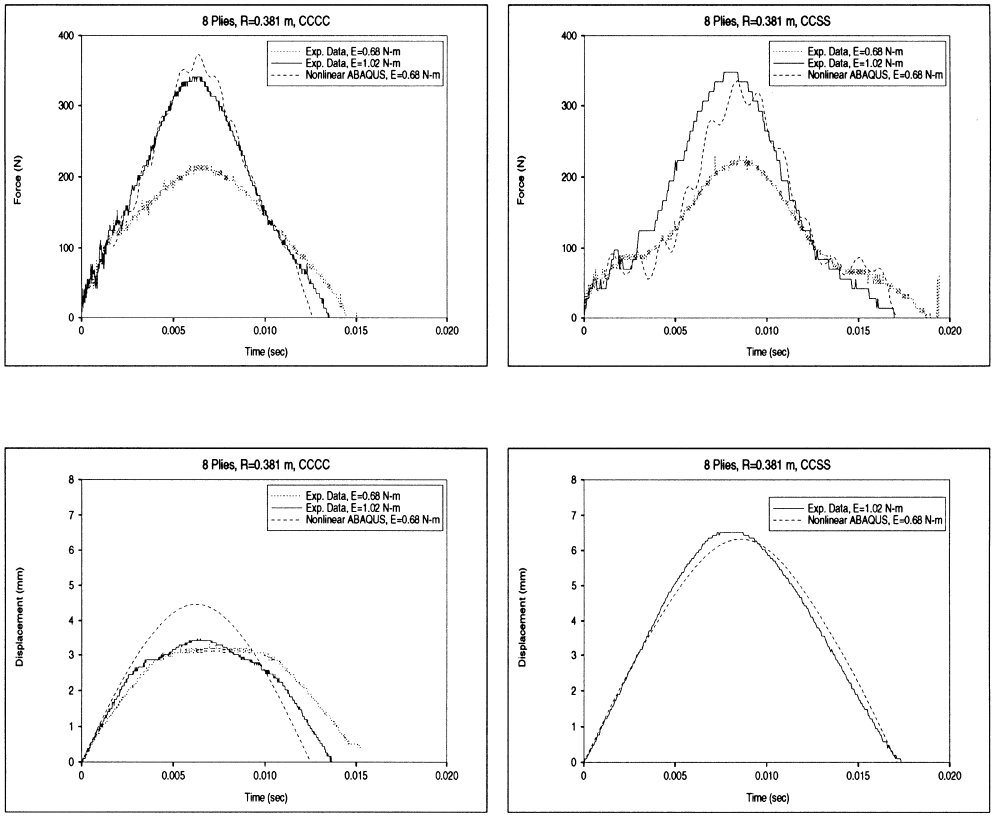

Fig. 9. Out of plane boundary effect on response histories.

The influence of in-plane and out-of-plane boundary condition has been introduced for some of the cases in the test matrix. The influence of the boundary conditions on the other cases is reported in Kistler (1996). Careful consideration of the static force-displacement response sensitivity to in-plane and out-of-plane boundary conditions can facilitate the analysis of a range of supports used in experimental impact tests.

5. Concluding remarks

Static force-displacement curves for curved laminated panels were presented in order to provide insight into the corresponding experimentally observed impact response. The influence of panel curvature, thickness, in-plane and out-of-plane edge boundary conditions and the validity of linear and nonlinear curved plate theory, especially in the context of impact, was investigated. As the thickness decreases, deformations increase and curvature effects become increasingly important. As the curvature was varied, a structural response behavior similar to the limit-point instability of an arch was found. The more curved panels incurred stronger limit-point characteristics which

lead to a softening of the force-displacement curve. Flatter panels responded to impact with larger peak forces than more curved panels, as well as smaller peak displacements and contact durations. Because the nonlinear analyses properly accounted for both large bending deformations and in-plane membrane effects this behavior was accurately predicted and is in agreement with experimental observation. Correlation of the large deformation dynamic response with nonlinear static force-displacement curves also provided insight toward understanding the influence of in-plane and out-of-plane boundary conditions on the impact response. This study establishes the importance of properly accounting for bending and membrane effects in a nonlinear setting for the study of curved plate impact, and shows that these effects are more dominant than inertia effects in the range of impact velocities and impact energies examined herein.

Acknowledgements

The authors are grateful for the financial support provided through the NASA Graduate Student Researcher's Program, NGT-50977, and the Department of Aerospace Engineering, University of Michigan. Furthermore, we acknowledge with thanks Dr D. Ambur, Technical Monitor, and Dr C. Prasad of the Aircraft Structures branch at NASA Langley Research Center for their guidance and use of facilities for the experimental impact tests. Computing services were provided by the Center for Parallel Computing at the University of Michigan which is partially funded by NSF grant CDA-92-14296.

References

Ambur, D. R., Starnes, J. H. and Prasad, C. B. (1993) Influence of transverse shear and large-deformation effects on the low-speed impact response of laminated composite plates, NASA TM 107753.

Kistler, L. S. (1996) Low Velocity Impact on Curved Laminated Composite Panels, Ph.D. Thesis, Dept. of Aerospace Engineering, University of Michigan, Ann Arbor, MI.

Kistler, L. S. (1994) Experimental Investigation of the Impact Response of Cylindrically Curved Laminated Composite Panels, *AIAA/ASME/ASCE/AHS/ASC 35th Structures, Structural Dynamics, and Materials Conference*, AIAA-94-1604-CP.

Kistler, L. S. and Waas, A. M. (1997a) Experiment and Analysis on the Response of Curved Laminated Composite Panels Subjected to Low Velocity Impact, University of Michigan Aerospace Engineering Report SM 96-19, submitted to *International Journal of Solids and Structures*.

Kistler, L. S. and Waas, A. M. (1997b) Impact Response of Cylindrically Curved Laminates Including a Large Deformation Scaling Study, University of Michigan Aerospace Engineering Report SM 96-21, submitted to *International Journal of Impact Engineering*.

Lagace, P. A. and Wolf, E. (1995) Impact damage resistance of several laminated material systems, *AIAA Journal* **33**(6), 1106–1113.

Matsuhashi, H., Graves, M. J., Dugundji, J. and Lagace, P. A. (1993) Effect of membrane stiffening in transient impact analysis of composite laminated panels, Proc. 34 AIAA/ASME/ASCE/AHS/ASC SDM, AIAA Hq., Washington, DC, 2668–2678.

Murphy, D. (1994) Nonlinear analysis provides new insights into impact damage of composite structures, *Composites* **25**(1), 65–69.

Prasad, C. B., Ambur, D. R. and Starnes, J. H. (1994) Response of laminated composite plates to low-speed impact by different impactors, *AIAA Journal* **32**(6), 1270–1277.

Sun, C. T. and Chattopadhyay, S. (1975) Dynamic response of anisotropic laminated plates under initial stress to impact of a mass, *J. Applied Mechanics* Sept. 1975, 693–698.